TransformerLess Partial Voltage DC-DC Converter with Safety-Oriented Control for Green Hydrogen Production

Diego Concha[1], Thierry Meynard[1], Maurice Fadel[1], Ana Llor[1], Henri Schneider[1]
Hugues Renaudineau[2], Samir Kouro[3], Javier Solano[4]
[1]LAPLACE CNRS-INPT-UPS, Université de Toulouse
[2]Universidad San Sebastian, Valdivia, Chile
[3]Department of Electronic Engineering, Universidad Tecnica Federico Santa Maria, Valparaiso, Chile
[4]European Institute for Energy Research, Karlsruhe, Germany

Abstract – A safety control strategy for the TransformerLess Partial Voltage Converter (TLPVC) applied to green hydrogen production via water electrolysis is proposed. Given the narrow operational voltage range of electrolyzers, the TLPVC presents a suitable solution by processing only a fraction of the input voltage while effectively covering the full voltage range required by the electrolyzers. In addition, the TLPVC improves the Semiconductor Capacity Utilization Index (SCUI) by reducing the stress on the switching cells, enabling more efficient power handling compared to conventional buck DC-DC converters. Its structure enables current balancing between electrolyzers using a single duty cycle. However, due to electrolyzer aging, parameter variations may arise over time, potentially causing imbalances in the input capacitor voltages—especially at higher duty cycles. To address this, a nonlinear safety-oriented control strategy is proposed, regulating the current of the most degraded electrolyzer while maintaining balanced input capacitor voltages. Simulation results obtained using PLECS confirm the effectiveness of the proposed approach.

Keywords – DC-DC converter, Electrolyzer, Capacitor Voltage Balance, TransformerLess Partial Voltage Converter.

1. INTRODUCTION

Hydrogen production systems have gained significant attention due to the versatility of hydrogen as an energy carrier. With an exceptional energy density of 140 MJ/kg—more than twice that of conventional fuels—hydrogen offers a means to store excess renewable energy and provide a stable energy supply when needed [1]. Beyond its conventional use as an industrial feedstock in refining and chemical production, hydrogen also enables the synthesis of e-fuels such as e-ammonia, e-methanol, and e-kerosene, which are critical for decarbonizing hard-to-abate sectors [2].

Producing hydrogen from renewable energy–referred to as green hydrogen–is an increasingly attractive pathway for sustainable energy transition. However, achieving this goal presents several technical challenges. One key step is the water electrolysis process, in which water molecules are split into hydrogen and oxygen using a stable DC current, typically supplied by power electronic converters. Since the DC current is directly proportional to the hydrogen production rate [3], there is a growing trend toward increasing the power capacity of electrolyzers, reaching tens of megawatt. Global cumulative electrolyzer capacity is projected to reach 4.5 TW by 2050 [4].

DC-DC converters are the interface between a DC-link and the electrolyzers. The trend is to further increase the installed capacity of these devices, presenting challenges from the power electronics perspective. For DC-coupled electrolyzer, isolated, as the dual active bridge, or non-isolated, as the classic buck converter, have been largely proposed in the literature [5]. As the DC-link voltage has been increasing in rating to reduce

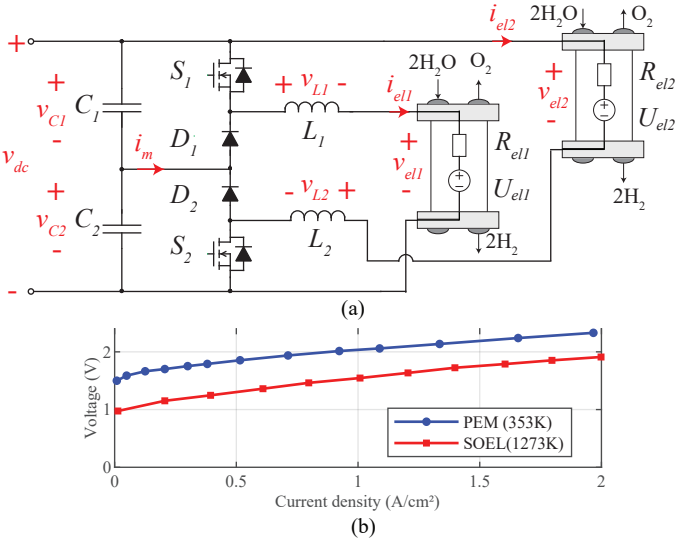

Figure 1. TransformerLess Partial Voltage Converter (TLPVC) for Green Hydrogen production. (a) Topology. (b) Polarization curve of the electrolyzers: Proton Exchange Membrane (PEM) and Solid Oxide Electrolysis (SOEL) [13].

power losses, switches in these DC-DC converters must handle higher input voltages, increasing the electrical stress, so multilevel DC-DC converter to divide the electrical voltage stress can be adapted to these systems [17]. To support higher power demands, modular hydrogen production architectures are being explored, with DC-DC converters playing a key role in decentralizing power conversion and adapting voltage and current levels to meet the requirements of multi-stack electrolyzer systems. For example, in [6], a modular three-level buck converter is proposed to feed three electrolyzers.

DC-DC Partial Power Converters (PPCs) offer an efficient solution by processing only a fraction of the total power [7]. They have been proposed for various applications, including electric vehicles [8], photovoltaics [9], fuel-cell systems [10], and electrolyzers [11]. PPC architectures focus on processing only the necessary portion of power, thereby reducing converter stress and improving overall efficiency [8]. This makes them attractive for optimized power conversion systems. However, most PPCs include high-frequency transformers, which add cost, volume, and limit power density. TransformerLess PPCs thus offer a promising alternative [8].

Given the narrow operating voltage range of electrolyzers

[12], a DC-DC converter that processes only a fraction of the input voltage–while still meeting the electrolyzers voltage requirements–can be highly effective. The TransformerLess Partial Voltage Converter (TLPVC) topology is capable of supplying two electrolyzers, each operating only within the upper segment of the available input voltage range, rather than requiring the full span from zero to maximum voltage, as is the case with conventional buck DC-DC converters, such as the classic buck.

An important advantage of the TLPVC is SCUI, which is defined as the power transferred from one side of the converter to the other, divided by the product of the peak voltage and the peak current of the semiconductors. Higher SCUI indicates better semiconductor utilization, leading to a more cost-effective solution with capability of converting higher power with the same components, or smaller components for equal application. For traditional DC-DC converters, the SCUI varies between [0;1] but for TLPVCs it is between [1;2] depending on the operating point. Another important feature of the TLPVC is its ability to balance current between two branches using a single duty cycle. However, over time, electrolyzer aging can lead to parameter mismatches, resulting in voltage imbalance across the input capacitors. This may cause unacceptable differences in blocking voltage between the switching cells. If one electrolyzer degrades more than the other, active control is required to maintain safe and efficient operation.

This article proposes a safety-oriented control strategy that ensures current limitation and balanced input capacitor voltages, even in the presence of degraded or mismatched electrolyzers. By regulating only two switches, the method maintains voltage balance across the switching cells and prioritizes current regulation for the most degraded electrolyzer. The proposed strategy guarantees safe operation while preventing current overshoot in either branch.

The article is structured as follows: Section 2 introduces the concept and operating principles of the proposed topology. Section 3 defines and analyzes the Semiconductor Capacity Utilization Index. Section 4 details the control strategy developed for the TLPVC. Simulation results are shown in Section 5, and conclusion is presented in Section 6.

2. CONCEPT AND TOPOLOGY DESCRIPTION

Fig. 1(a) shows the proposed TLPVC topology composed by two switching cells and two electrolyzers, connected to a fraction of the input voltage. Fig. 1(b) shows the polarization curve of electrolyzers [13]. As can be seen, electrolyzers operate within a narrow operational voltage range, approximately from 50% to 100% of their maximum operational voltage. For modelling, electrolyzer behaviour can be represented by a internal resistance with a series voltage source. To efficiently meet this requirement, the TLPVC processes only a fraction of the input voltage, which is sufficient to cover the entire voltage range of the electrolyzers. The input voltage of the DC-link is defined as v_{dc}, while v_{el1} and v_{el2} are the voltage of electrolyzer 1 and 2, respectively. The parameters R_{el1} and U_{el1} are the model parameters of electrolyzer 1 and R_{el2} and U_{el2} are the model parameters of electrolyzer 2.

By using the average model analysis, the electrolyzer's voltages can be defined as

$$\begin{aligned} v_{el1} &= v_{C2} + d_1 v_{C1}, \\ v_{el2} &= v_{C1} + d_2 v_{C2}, \end{aligned} \tag{1}$$

where d_1 is the duty cycle for switch S_1 and d_2 is the duty cycle for switch S_2.

Assuming equal electrolyzer's parameters and fixed input voltage, the electrolyzer's voltages can be defined as

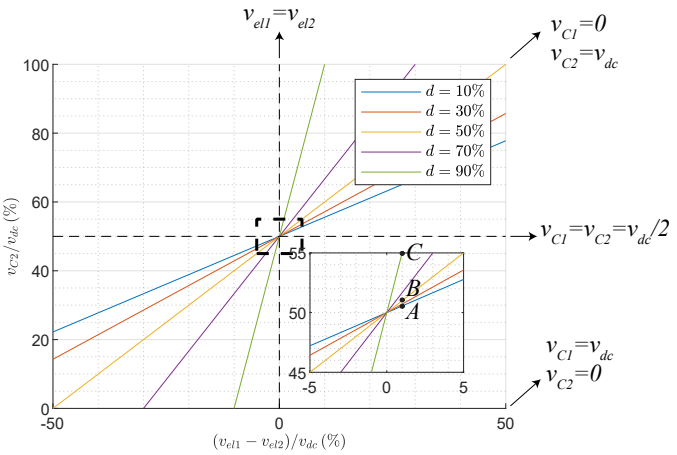

Figure 2. Evolution of normalized midpoint voltage vs electrolyzer unbalance.

$$\begin{aligned} v_{el1} &= \frac{v_{dc}}{2} + d_1 \frac{v_{dc}}{2}, \\ v_{el2} &= \frac{v_{dc}}{2} + d_2 \frac{v_{dc}}{2}. \end{aligned} \tag{2}$$

In these equations, the "partiality" concept can be appreciated: if $d_1 = 0$, $v_{el1} = v_{dc}/2$ and if $d_1 = 1$, $v_{el1} = v_{dc}$, comprising only the voltage fraction operation region ($v_{dc}/2$, v_{dc}). Same analysis can be replicated for v_{el2} voltage.

The current i_m, in steady-state, can be expressed as

$$i_m = (1 - d_1)\, i_{el1} - (1 - d_2)\, i_{el2}, \tag{3}$$

where i_{el1} and i_{el2} are the currents through electrolyzer 1 and 2, respectively. Imposing the same duty cycles on S_1 and S_2, the average value of i_m becomes near of 0, results in the same average current for both electrolyzers, independent of the model parameters of both electrolyzers.

Thanks to the average model, four equations are derived,

$$v_{dc} - (U_{el2} + R_{el2} i_{el2}) - (1 - d_2) v_{C2} = 0, \tag{4}$$

$$v_{dc} - (U_{el1} + R_{el1} i_{el1}) - (1 - d_1) v_{C1} = 0, \tag{5}$$

$$i_m = (1 - d_1) i_{el1} - (1 - d_2) i_{el2} = 0, \tag{6}$$

$$v_{dc} = v_{C1} + v_{C2}, \tag{7}$$

where d_1 , d_2, v_{C1} and v_{C2} are the incognites. Making the difference of (4) and (5), and assuming $d_1 = d_2 = d$,

$$\Delta v_C = v_{C1} - v_{C2} = \frac{U_{el2} - U_{el1} + i_{el}(R_{el2} - R_{el1})}{1 - d}, \tag{8}$$

$$\Delta v_C = v_{C1} - v_{C2} = \frac{v_{el2} - v_{el1}}{1 - d}. \tag{9}$$

If the electrolyzer parameters are identical, i.e., $R_{el1} = R_{el2}$ and $U_{el1} = U_{el2}$, the input capacitor voltages remain balanced, with $v_{C1} = v_{C2} = v_{dc}/2$, regardless of the duty cycle d. However, any mismatch in resistance or voltage offset between the electrolyzers leads to a deviation from this balance. This effect becomes more pronounced as d approaches 1, where even small parameter differences result in significant voltage imbalance between v_{C1} and v_{C2}.

Adding (7) and (9) yields,

$$(v_{C1} - v_{C2}) + (v_{C1} + v_{C2}) = \frac{v_{el2} - v_{el1}}{1-d} + v_{dc}, \tag{10}$$

$$2v_{C1} = v_{dc} + \frac{v_{el2} - v_{el1}}{1-d}, \tag{11}$$

$$v_{C1} = \frac{1}{2}\left(v_{dc} + \frac{v_{el2} - v_{el1}}{1-d}\right). \tag{12}$$

Substituting into (7) and solving for v_{C2},

$$v_{C2} = v_{dc} - v_{C1}, \tag{13}$$

$$= \frac{1}{2}v_{dc} - \frac{1}{2}\cdot\frac{v_{el2} - v_{el1}}{1-d}, \tag{14}$$

$$v_{C2} = \frac{1}{2}\left(v_{dc} + \frac{v_{el1} - v_{el2}}{1-d}\right). \tag{15}$$

Fig. 2 shows the evolution of normalized v_{C2} voltage in function of the electrolyzer voltage unbalance for different duty cycle values assuming $d_1 = d_2 = d$. The sensitivity of the capacitor midpoint to unbalanced electrolyzer voltages increases as the duty cycle approaches 100%. This behavior can be explained by the fact that, under high duty cycle conditions, the diodes D_1 and D_2, which clamp the capacitor voltages to the midpoint, are rarely conducting. As a consequence, the voltage balancing between the two branches is no longer actively enforced by the diodes. Instead, the system relies on the natural redistribution of the capacitor voltages to passively compensate for differences in the electrolyzer voltages.

Points A, B, and C in Fig. 2 illustrate the impact of a 1% mismatch between the electrolyzer voltages, i.e., $(v_{el1} - v_{el2})/v_{dc} = 1\%$, for three different duty cycles: 10%, 50%, and 90%, respectively. This small deviation in the electrolyzer voltages results in different levels of voltage imbalance at the midpoint, represented by v_{C2}/v_{dc}, depending on the duty cycle. Specifically, the corresponding deviations from the balanced point (50%) are approximately 0.55% for point A ($d = 10\%$), 1% for point B ($d = 50\%$), and 5% for point C ($d = 90\%$). These results confirm that under high duty cycle conditions, the system becomes more sensitive to small mismatches in the electrolyzer voltages, leading to a stronger deviation in the midpoint voltage.

3. SCUI DEFINITION

SCUI can be defined as the ratio between the power transferred from one side of the converter to the other, and the product of the peak voltage and peak current handled by the semiconductors. Introduced in [15], a higher SCUI reflects better utilization of the semiconductor devices, leading to more cost-effective solution of semiconductors and enabling either higher power transfer with the same components or the use of smaller components for the same application.

A briefly comparison with conventional buck converters is explained, being BC refered to buck converter [16] and DBC refered to Dual Buck Converter [17]. When multiple switching cells and/or multiple low-voltage sources are involved–two low voltage sources for TLPVC–, the total power transferred (assuming 100% efficiency and negligible ripple) is evaluated as the absolute value of the sum of the average powers of the sources on one side of the converter. This is then divided by the sum of the average voltage-current products corresponding to each switching cell,

$$SCUI = \frac{\sum_j |\vec{v}_{LV,j}\vec{i}_{LV,j}|}{\sum_k |\vec{v}_k\vec{i}_k|}, \tag{16}$$

where:

- $\vec{v}_{LV,j}$ and $\vec{i}_{LV,j}$ are the average voltage and current of the j-th low-voltage source:
  - For BC: $\vec{v}_{LV,1} = dv_{dc}$ and $\vec{i}_{LV,1} = i_{el}$.
  - For DBC: $\vec{v}_{LV,1} = dv_{dc}$ and $\vec{i}_{LV,1} = i_{el}$.
  - For TLPVC: $\vec{v}_{LV,1} = \vec{v}_{LV,2} = d\frac{v_{dc}}{2} + \frac{v_{dc}}{2}$ and $\vec{i}_{LV,1} = \vec{i}_{LV,2} = i_{el}$.
- $\vec{v}_k$ and $\vec{i}_k$ are the peak voltage and current across the k-th switching cell:
  - For BC: $\vec{v}_1 = v_{dc}$ and $\vec{i}_1 = i_{el}$.
  - For DBC: $\vec{v}_1 = \vec{v}_2 = \frac{v_{dc}}{2}$ and $\vec{i}_1 = \vec{i}_2 = i_{el}$.
  - For TLPVC: $\vec{v}_1 = \vec{v}_2 = \frac{v_{dc}}{2}$ and $\vec{i}_1 = \vec{i}_2 = i_{el}$.
- j indexes the number of low-voltage sources:
  - $j = 1$ for BC and DBC.
  - $j = 1, 2$ for TLPVC.
- k indexes the number of switching cells:
  - $k = 1$ for BC.
  - $k = 1, 2$ for DBC and TLPVC.

Given this definition, the SCUI is not strictly a characteristic of the converter topology itself—it also depends on the operating point. Thus, the range of SCUI in DC-DC converters becomes more comprehensible. For example, in BC, the semiconductors switch the full input voltage v_{dc} and conduct the electrolyzer current i_{el}, so the SCUI becomes

$$SCUI = \frac{(dv_{dc})i_{el}}{v_{dc}i_{el}} = d, \quad \text{with } 0 \le d \le 1. \tag{17}$$

For the DBC, which is composed by two switching cells, but only one low-voltage source (one electrolyzer) the SCUI is

$$SCUI = \frac{(dv_{dc})i_{el}}{2\left(\frac{v_{dc}}{2}i_{el}\right)} = d, \quad \text{with } 0 \le d \le 1. \tag{18}$$

For the TLPVC, which is composed by two switching cells and two low voltage sources (two electrolyzers), the SCUI is calculated as

$$SCUI = \frac{2\left(d\frac{v_{dc}}{2} + \frac{v_{dc}}{2}\right)i_{el}}{2\left(\frac{v_{dc}}{2}i_{el}\right)} = d+1, \quad \text{with } 0 \le d \le 1. \tag{19}$$

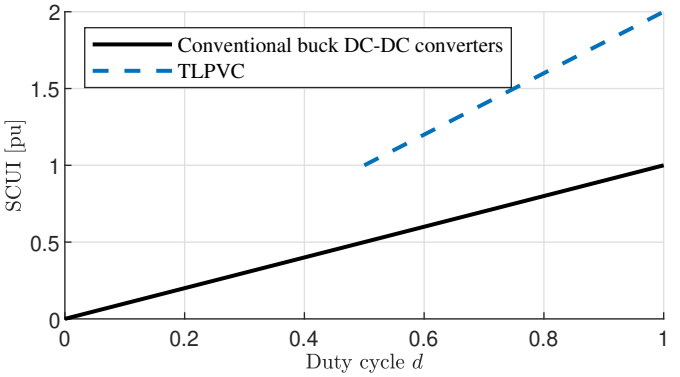

Figure 3. Semiconductor Capacity Utilization Index (SCUI) in conventional buck DC-DC converters and TLPVC.

Fig. 3 shows the SCUI [pu], comparing the range of conventional buck DC-DC converters, which ranges between [0, 1], with that of the TLPVC, where the SCUI can extend from [1, 2]. In other words, the SCUI in the TLPVC reflects a more efficient use of the semiconductors for power transfer to the loads and ensures a partial voltage operation [15].

4. CLOSED-LOOP CONTROL SCHEME

In the TLPVC topology, only two switches (S_1 and S_2) are active, while three variables must be regulated in the case of unbalanced condition: the electrolyzer currents i_{el1} and i_{el2}, and the input capacitor voltage balance, defined as the voltage difference $\Delta v_C = v_{C1} - v_{C2}$. As analyzed in the previous section, under ideal balanced conditions and assuming identical electrolyzer parameters, open-loop operation with equal duty cycles can ensure $\Delta v_C \approx 0\,\text{V}$, thereby eliminating the need for closed-loop control. However, in practical scenarios, electrolyzers may experience aging and degradation at different rates, leading to parameter mismatches. This variability poses a significant challenge for the TLPVC, as maintaining balanced condition becomes non-trivial. To address this, a control strategy can be proposed that prioritizes the current of the more degraded electrolyzer (i_{el1} or i_{el2}), while actively regulating the midpoint voltage deviation Δv_C. The most degraded electrolyzer is taken into account by measuring the maximum current. This control approach ensures safe and stable operation under non-ideal conditions.

The objective of the safety control strategy is to ensure that currents do not exceed the reference, regulating, at least, one of the two electrolyzer currents. In this analysis, only variations in internal resistance between the two electrolyzers are considered, i.e., $R_{el1} \neq R_{el2}$, while the reversible voltage is assumed to be constant and equal for both electrolyzers: $U_{el1} = U_{el2} = U_{el}$.

Based on this assumption, the current dynamics for both electrolyzers can be expressed as follows,

$$L_1 \frac{di_{el1}}{dt} = -R_{el1} i_{el1} + v_{C2} - U_{el} + v_{C1} d_1, \tag{20}$$

$$L_2 \frac{di_{el2}}{dt} = -R_{el2} i_{el2} + v_{C1} - U_{el} + v_{C2} d_2. \tag{21}$$

Focusing on the current dynamics of i_{el1} and isolating the control input d_1, the following control law is obtained,

$$d_1 = \frac{L_1 \frac{di_{el1}}{dt} + R_{el1} i_{el1} - v_{C2} + U_{el}}{v_{C1}}. \tag{22}$$

To simplify the control implementation, the term $L_1 \frac{di_{el1}}{dt} + R_{el1} i_{el1}$ is grouped and denoted as δ, which represents the output of the PI controller (including both dynamic and resistive compensation). Thus, the control law becomes,

$$d_1 = \frac{\delta - v_{C2} + U_{el}}{v_{C1}}. \tag{23}$$

The safety control of the TLPVC can be implemented in two ways: either by estimating the internal resistances of the electrolyzers, if possible (and selecting the one with the highest resistance), or by identifying the electrolyzer with the highest actual current demand and using it as the reference for current control. In both cases, the objective is to ensure that the system tracks the most demanding electrolyzer while maintaining the current of the other one below or equal to it.

Consequently, the inverse function used in the control law must be adapted accordingly. Instead of using the respective voltage and resistance values of a specific electrolyzer, the worst-case conditions must be considered. The modified control law is expressed as,

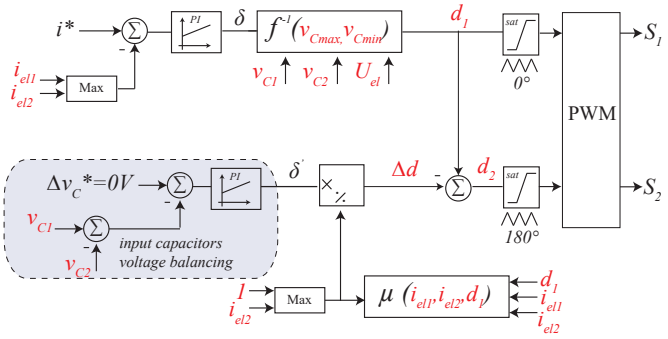

Figure 4. Proposed safety control scheme for TLPVC, including current control of the most degraded electrolyzer plus voltage balancing control on the input capacitors.

$$d_1 = \frac{\delta - v_{Cmin} + U_{el}}{v_{Cmax}}, \tag{24}$$

where v_{Cmin} and v_{Cmax} represent, the minimum and maximum capacitor voltages, respectively. This conservative design ensures safe operation across all operating conditions, even in the presence of parameter mismatches or aging effects.

Once the current loop to pilot the maximum of i_{el1} or i_{el2} is analyzed, the other variable to control is Δv_C. The midpoint potential can be influenced by changing the equality of the two duty cycles and the current i_m plays a key role in controlling this midpoint. Assuming $C_1 = C_2 = C$ and considering the voltage difference, is possible to define,

$$\Delta v_C = v_{C1} - v_{C2}. \tag{25}$$

The dynamic equation governing the midpoint potential can be expressed as

$$C \frac{d\Delta v_C}{dt} = i_{el1}(1 - d_1) - i_{el2}(1 - d_2). \tag{26}$$

The difference between the two duty cycles is defined as

$$\Delta d = d_1 - d_2. \tag{27}$$

Substituting this definition into the previous equation yields,

$$C \frac{d\Delta v_C}{dt} = (1 - d_1)(i_{el1} - i_{el2}) - i_{el2} \Delta d. \tag{28}$$

This relationship expresses a non-linear behavior "affine in the control", of the form,

$$C \frac{d\Delta v_C}{dt} = g(z) + h(z) \Delta d. \tag{29}$$

where z is the state vector, as proposed in [14]. The functions $g(z)$ and $h(z)$ are defined as

$$g(z) = (1 - d_1)(i_{el1} - i_{el2}), \tag{30}$$

$$h(z) = -i_{el2}. \tag{31}$$

To linearize the system with respect to a new control input δ', a decoupling control law is proposed,

$$\Delta d = \mu(z) + \beta(z) \delta'. \tag{32}$$

Imposing the desired linear behavior,

$$C \frac{d\Delta v_C}{dt} = \delta'. \tag{33}$$

and substituting the control law into the affine form, is possible to obtain,

Table 1. Simulation Parameters.

Parameter	Value
Input voltage v_{dc}	200 V
Switching frequency f_s	20 kHz
Inductors $L_1 = L_2$	1 mH
$C_1 = C_2$	3300 μF
Resistance parameter $R_{el1} = R_{el2}$	2.97 Ω
Voltage source parameter $U_{el1} = U_{el2}$	136.8 V

$$g(z) + h(z)\mu(z) + h(z)\beta(z)\delta' = \delta'. \tag{34}$$

To ensure that this equation holds for any δ', is required that,

$$g(z) + h(z)\mu(z) = 0, \tag{35}$$

$$h(z)\beta(z) = 1. \tag{36}$$

Solving for $\mu(z)$ and $\beta(z)$ yields,

$$\mu(z) = -h^{-1}(z)g(z), \tag{37}$$

$$\beta(z) = h^{-1}(z). \tag{38}$$

Assuming $i_{el2} \neq 0$, which ensures the existence of $h^{-1}(z)$, the control law becomes,

$$\mu = \frac{(1 - d_1)(i_{el2} - i_{el1})}{i_{el2}}, \tag{39}$$

$$\beta = -\frac{1}{i_{el2}}. \tag{40}$$

Fig. 4 presents the proposed safety control scheme for the TLPVC. For comparison, imposing the same duty cycle on both S_1 and S_2 allows direct regulation of both electrolyzer currents (i_{el1} and i_{el2}). This approach is straightforward and enables current maximization, assuming the same v_{dc} for both control strategies. However, at high duty cycles, this method may lead to voltage imbalance across the input capacitors (see Fig. 2), potentially resulting in asymmetric stress on the power semiconductors. In contrast, the proposed safety control prioritizes the current regulation of the most degraded electrolyzer—typically the one with the highest internal resistance—while simultaneously controlling the midpoint voltage Δv_C. Although this strategy involves increased implementation complexity, it ensures improved voltage symmetry across the switching devices and enhances the overall reliability of the system in the long term, while ensuring that the two currents do not become higher than the reference.

5. SIMULATION RESULTS

Table 1 summarizes the simulation parameters. The electrolyzer behavior is modeled by the equation $v_{el} = 136.8\,\text{V} + 2.97\,i_{el}$. Fig. 5 presents the simulation results of the proposed closed-loop safety control scheme. Fig. 5(a) shows the input capacitor voltages v_{C1} and v_{C2}, Fig. 5(b) depicts the electrolyzer currents i_{el1} and i_{el2}, and Fig. 5(c) shows the variation of the resistance R_{el1}. From $t = 0\,\text{s}$ to $t = 0.03\,\text{s}$, the electrolyzer parameters are identical, i.e., $R_{el1} = R_{el2}$ and $U_{el1} = U_{el2}$. Consequently, the input capacitor voltages are balanced at 50%–50%, as expected. The current reference is maintained at $i^* = 4\,\text{A}$ throughout the entire simulation. At $t = 0.03\,\text{s}$, R_{el1} increases by 20% with respect to R_{el2}, which retains its nominal value. Since electrolyzer 1 is more degraded than electrolyzer 2, the control loop prioritizes the regulation of i_{el1}. At this stage, the input capacitor voltages are also regulated, fulfilling the control loop objective.

Fig. 6 presents another simulation scenario, where R_{el1} increases first, followed by a greater increase in R_{el2}, with

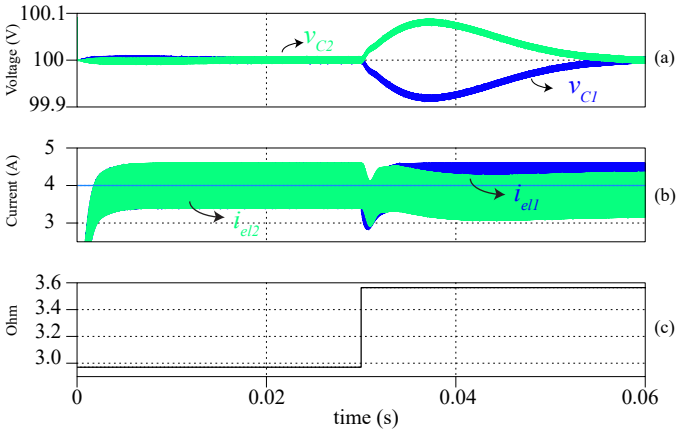

Figure 5. Simulation results of the proposed safety control in TLPVC. (a) input capacitor voltages v_{C1} and v_{C2}. (b) electrolyzer currents i_{el1} and i_{el2}. (c) variation of R_{el1} from 2.97Ω to 3.564Ω.

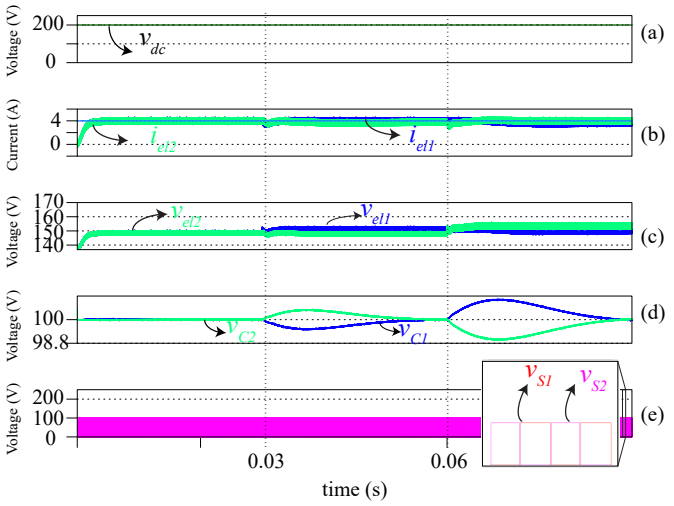

Figure 6. Simulation results of the proposed safety control in TLPVC. (a) input voltage v_{dc}. (b) electrolyzer currents i_{el1} and i_{el2}. (c) electrolyzer voltages v_{el1} and v_{el2}. (d) input capacitor voltages v_{C1} and v_{C2}. (e) switches voltages v_{S1} and v_{S2}.

$i^* = 4\,\text{A}$. Fig. 6(a) shows the input voltage v_{dc}, Fig. 6(b) displays the electrolyzer currents i_{el1} and i_{el2}, Fig. 6(c) shows the electrolyzer voltages v_{el1} and v_{el2}, Fig. 6(d) shows the input capacitor voltages v_{C1} and v_{C2}, and Fig. 6(e) illustrates the switch voltages v_{S1} and v_{S2}. Before $t = 0.03\,\text{s}$, the system is balanced, with input capacitor voltages at 100 V, corresponding to half of the input voltage $v_{dc} = 200\,\text{V}$. At $t = 0.03\,\text{s}$, R_{el1} increases by 20% relative to R_{el2}, prompting the controller to regulate i_{el1} at 4 A. During this interval, i_{el2} is not actively controlled and assumes a value lower than the reference. At $t = 0.06\,\text{s}$, R_{el2} increases by 40% with respect to the nominal value of 2.97 Ω, while R_{el1} remains 20% above nominal—effectively inverting the degradation condition. From this point on, the controller shifts its regulation to i_{el2}, maintaining it at 4 A. Since electrolyzer voltages are proportional to their respective currents, their waveforms follow the same trend, as shown in Fig. 6(b) and Fig. 6(c). Throughout the simulation, the input capacitor voltages remain regulated at 100 V, ensuring that the blocking voltages of switches S_1 and S_2 do not exceed this value—corresponding to the voltages across capacitors C_1 and C_2.

6. CONCLUSION

A safety-oriented control scheme has been proposed for the TransformerLess Partial Voltage Converter (TLPVC) applied to green hydrogen production systems based on electrolyzers. The proper operation of the converter relies on the assumption of identical electrolyzer parameters. However, significant parameter deviations—resulting from aging or degradation—can lead to imbalances in the input capacitor voltages, which in turn cause unequal voltage blocking across the switching cells. To mitigate this issue, a control strategy is implemented that regulates the current of the most degraded electrolyzer while simultaneously ensuring voltage balancing of the input capacitors. Simulation results validate the effectiveness of the proposed scheme in maintaining input voltage balance under electrolyzer degradation conditions.

7. ACKNOWLEDGMENTS

This work was supported by the Agencia Nacional de Investigacion y Desarrollo of Chile (ANID) through grants AC3E (ANID/BASAL/AFB240002), FONDECYT Iniciacion grant 11240917, and SERC Chile (ANID/FONDAP/1523A0006). The work was also supported by the European Institute for Energy Research (EIFER).

8. REFERENCES

[1] J. Chi and H. Yu, “Water electrolysis based on renewable energy for hydrogen production,” Chinese Journal of Catalysis, vol. 39, no. 3, pp. 390–394, 2018. doi: 10.1016/S1872-2067(17)62949-8

[2] Nemmour, Amira & Inayat, Abrar & Janajreh, Isam & Ghenai, Chaouki. (2023). Green hydrogen-based E-fuels (E-methane, E- methanol, E-ammonia) to support clean energy transition: A literature review. International Journal of Hydrogen Energy.10.1016/j.ijhydene.2023.03.240.

[3] Schmidt, P., Zittel, W., Weindorf, W., Rakasha, T., Goericke, D. (2016). Renewables in transport 2050 – Empowering a sustainable mobility future with zero emission fuels. In: Bargende, M., Reuss, HC., Wiedemann, J. (eds) 16. Internationales Stuttgarter Symposium. Proceedings. Springer, Wiesbaden.

[4] Infineon Technologies AG, Green hydrogen: Efficient electrolysis through comprehensive power conversion solutions, 2022.

[5] D. Guilbert, S. M. Collura, and A. Scipioni, "DC/DC converter topologies for electrolyzers: State-of-the-art and remaining key issues," Int. J. Hydrogen Energy, vol. 42, no. 38, pp. 23966–23985, 2017.

[6] S. Udomkaew, K. Sengsui, W. Saksiri, M. Phattanasak, R. Gavagsaz-Ghoachani and S. Pierfederici, "Two-Output Three-Level Buck Converter: Current Control with Capacitors Voltage Balancing Control," 2023 Research, Invention, and Innovation Congress: Innovative Electricals and Electronics (RI2C), Bangkok, Thailand, 2023, pp. 370- 374, doi: 10.1109/RI2C60382.2023.10355984.

[7] N. G. F. dos Santos, J. R. R. Zientarski, and M. L. da Silva Martins, “A review of series-connected partial power converters for dc–dc applications,” IEEE Journal of Emerging and Selected Topics in Power Electronics, vol. 10, no. 6, pp. 7825–7838, 2022.

[8] J. Anzola, I. Aizpuru, A. Arruti, J. S. Artal-Sevil, and C. Bernal, “Demystifying non-isolated dc–dc topologies on partial power processing architectures,” Electronics, vol. 11, no. 3, p. 480, 2022.

[9] S. Rivera, J. Rojas, S. Kouro, P. W. Lehn, R. Lizana, H. Renaudineau, and T. Dragicevi ˇ c, “Partial-power converter topology of type ii for ´ efficient electric vehicle fast charging,” IEEE Journal of Emerging and Selected Topics in Power Electronics, vol. 10, no. 6, pp. 7839–7848, 2022.

[10] M. C. Mira, Z. Zhang, K. L. Jørgensen, and M. A. E. Andersen, “Fractional charging converter with high efficiency and low cost for electrochemical energy storage devices,” IEEE Transactions on Industry Applications, vol. 55, no. 6, pp. 7461–7470, 2019.

[11] M. S. Hernandez, H. Renaudineau, D. Concha, and A. M. Llor, “Series partial power pre-regulator for dcx-based stand-alone green hydrogen production,” in 2021 IEEE 30th International Symposium on Industrial Electronics (ISIE), 2021, pp. 1–6

[12] A. E. Samani, A. D’Amicis, J. D. M. De Kooning, P. Silva, and L. Vandevelde, "Grid balancing with a large-scale electrolyser providing primary reserve," in Proc. 8th Renewable Power Generation Conference (RPG), Shanghai, China, 2019, pp. 1–7.

[13] K. T. Jacob, "Regenerative energy system using high-temperature electrolyzer and fuel cell equipped with liquid metal electrodes," in *SIPS2011: Fray Int. Symp. on Metals and Materials Processing*, vol. 5, FLOGEN Stars Outreach, 2011, p. 81.

[14] D. Concha, T. Meynard, M. Fadel, H. Renaudineau, S. Kouro, A. M. Llor, H. Schneider, and J. Solano, “Safety control of TransformerLess Partial Voltage DC-DC Converter for hydrogen production,” manuscript submitted to the *64th IEEE Conference on Decision and Control (CDC)*, Rio de Janeiro, Brazil, Dec. 10–12, 2025. Submission no. 950.

[15] T. A. Meynard, H. Renaudineau, P. S. Canales, S. Kouro, D. C. Fuentes, A. Llor, M. Fadel, and H. Schneider, “Transformerless partial voltage dc-dc converter with double power processing capacity,” submitted to *IEEE Open Journal of the Industrial Electronics Society*, Regular paper, Manuscript ID: 25-OJIES-0133.R1, May 2025.

[16] V. Guida, D. Guilbert and B. Douine, "Candidate Interleaved DC-DC Buck Converters for Electrolyzers: State-of-the-Art and Perspectives," 2018 IEEE International Conference on Environment and Electrical Engineering and 2018 IEEE Industrial and Commercial Power Systems Europe (EEEIC / I&CPS Europe), Palermo, Italy, 2018, pp. 1-6, doi: 10.1109/EEEIC.2018.8494457.

[17] D. Concha et al., "Interleaved Dual Buck Converter for Low-Carbon Hydrogen Production: Electrolyzer Current Control and Input Capacitors Voltage Balancing," IECON 2024 - 50th Annual Conference of the IEEE Industrial Electronics Society, Chicago, IL, USA, 2024, pp. 1-6, doi: 10.1109/IECON55916.2024.10905714.